Journal of Operation and Automation in Power Engineering

vol. 12, no. Special Issue, Dec. 2024, Pages: 64-75

http://joape.uma.ac.ir

Research Paper

Enhancing Frequency Stability in Islanded Microgrids via Model Predictive Control

Anvar Ziyadullayevich Avlokulov [1,*], *Suhrob Ovlayev* [1], *Hussein Basim Furaijl* [2], *Muntadher Abed Hussein* [3], *Hassan Khalid Abozibid* [4], *Zainab Ali Nasir* [5], *Tahir Toma Farhan* [6], *Sarmad Jaafar Naser* [7], *Oybarchin Avlayeva* [1], *Oybek Yulchiyev* [1], and *Dilorom Normuminova* [1]

[1]*Tashkent state University of Economics, Tashkent, Uzbekistan.*
[2]*University of Al-Ameed, Karbala, Iraq.*
[3]*Department of Sciences, Al-Manara College, Maysan, Iraq.*
[4]*Al-Zahrawi University College, Karbala, Iraq.*
[5]*Al-Nisour University College, Nisour Seq. Karkh, Baghdad, Iraq.*
[6]*Mazaya University College, Nasiriyah, Iraq.*
[7]*Collage of Nursing, National University of Science and Technology, Dhi Qar, 64001, Iraq.*

Abstract— *This paper proposes a Model Predictive Control-based strategy for secondary load frequency control to enhance the dynamic performance of such systems. The proposed controller generates optimal control signals for dispatchable units to minimize frequency deviations induced by load and generation variability. A comprehensive microgrid model is developed, incorporating photovoltaic arrays, wind turbines, fuel cells, battery and flywheel energy storage systems, diesel generators, and electrolyzers. The dynamic behavior of each component is formulated using small-signal transfer functions, and the MPC is designed based on a constrained quadratic optimization problem that predicts and mitigates frequency deviations. Simulation results in MATLAB/Simulink demonstrate the superiority of the proposed MPC approach compared to conventional and intelligent controllers, including Ziegler–Nichols tuned PI, Fuzzy-PI, CPSO-PID, and CPSO-FOPID. The proposed controller achieved a maximum frequency deviation of 0.0052 pu, a settling time of 5.1 seconds, and an ITAE of 0.00024—outperforming all benchmarks in both steady-state and transient scenarios. Robustness under system parameter variations and load disturbances was also validated through five distinct case studies. The controller exhibits improved reliability, reduced stress on primary controllers, and better resilience to uncertainties. Future work will focus on implementing adaptive MPC algorithms, integrating machine learning-based disturbance predictors, and validating the control scheme using real-time hardware-in-the-loop platforms for enhanced applicability in hybrid AC/DC microgrids.*

Keywords—Model predictive control, secondary control, renewable energy integration, frequency oscillations, system stability, robust control, hardware in the loop validation.

1. INTRODUCTION

The increasing penetration of renewable energy sources into modern power systems has transformed the operational dynamics of electrical networks, particularly at the distribution level. Microgrids, as localized clusters of distributed generation units and controllable loads, are key enablers of this transformation due to their ability to operate independently from the main grid during disturbances. However, this operational autonomy introduces new technical challenges—most notably in maintaining system frequency stability under variable load and generation conditions. Traditional Load Frequency Control (LFC) strategies often fall short in addressing the nonlinearities and uncertainties inherent in microgrids powered by intermittent resources like wind and solar. As such, there is a growing need for advanced, model-based control frameworks capable of ensuring robust and adaptive frequency regulation. This paper addresses this need by developing a predictive control strategy tailored for frequency regulation in islanded microgrids with high renewable energy integration.

1.1. Research motivation

The escalating global demand for electrical energy poses significant challenges for the power industry. Among these challenges are the high capital investments required for constructing new power plants, expanding transmission and distribution networks, and addressing increasing environmental concerns due to climate change. To tackle these issues while enhancing reliability,

Received: 04 Apr. 2025
Revised: 03 Jul. 2025
Accepted: 10 Jul. 2025
*Corresponding author:
E-mail: umarovshukhratbadreddinovich@gmail.com (A.Z. Avlokulov)
DOI: 10.22098/JOAPE.2025.17113.2335

reducing power losses, and alleviating congestion in transmission lines, the integration of Distributed Generation (DG) [1] and renewable energy sources [2] has become an effective and evolving solution over the past two decades [3]. The notable benefits of these technologies have accelerated the development and deployment of microgrids in many regions around the world [4]. Microgrids small-scale power networks that incorporate various renewable energy sources and serve localized loads offer resilience and flexibility. Under typical operating conditions, microgrids are connected to the main grid, but during major disturbances or emergencies, they can operate in islanded mode to support critical loads. This operational flexibility, however, brings forth substantial technical challenges, particularly due to power variability from sources like wind and solar, and the dynamic behavior of connected loads. Among these challenges, the issue of frequency and power oscillations stands out, necessitating advanced control strategies to maintain system stability and performance [5]. Recent research has also explored the use of reinforcement learning (RL) for adaptive control in microgrids. A notable study presented a model-free, Q-learning-based supervisory controller designed to mitigate frequency and voltage oscillations in microgrids with high wind power penetration. By modeling the control environment as a Markov Decision Process (MDP), the proposed RL strategy demonstrated superior adaptability and dynamic performance compared to classical PID and fuzzy-PID controllers, particularly under uncertain and nonlinear conditions [6].

1.2. Literature review

The field of Load Frequency Control (LFC) in microgrids has attracted significant research attention due to the increasing integration of renewable energy sources and the resulting operational challenges. Numerous control strategies ranging from conventional methods to advanced predictive and heuristic techniques have been developed to address issues of frequency stability, power imbalance, and dynamic response in islanded microgrids. This subsection reviews recent and relevant contributions, highlighting their scope, limitations, and relevance to the development of the proposed Model Predictive Control (MPC) approach. Numerous studies have explored Load Frequency Control (LFC) in microgrids, which is critical to mitigating power imbalances and maintaining frequency within acceptable ranges. A comprehensive overview of such efforts is given in [7]. Generally, these studies fall into two categories: conventional control methods and metaheuristic-based techniques. In [8], a learning-based Tube-Based Robust Model Predictive Control (RMPC) approach is proposed for voltage regulation in islanded AC microgrids. By integrating Gaussian Process regression, the method adaptively adjusts the control tube to reduce conservatism under uncertainty. However, this work focuses solely on voltage control at the primary level and does not address frequency dynamics or system-level coordination. In contrast, our MPC-based Load Frequency Control (LFC) strategy operates at the secondary level, targeting system-wide frequency deviations by accounting for the interactions among diverse DERs and nonlinear loads under uncertainty. The study in [9] develops a Model Predictive Control framework integrated with a Two-Layer Moving Horizon Estimation (TL-MHE) observer for frequency regulation in PV-dominated microgrids. While effective for improving disturbance estimation and frequency recovery, the method is closely tied to VSG-based PV systems and lacks generalizability across mixed-source microgrids. Our work, by comparison, presents a generalized and RES-agnostic MPC-based frequency control scheme validated on a microgrid with PV, wind, fuel cells, and batteries, ensuring robust performance across diverse configurations.

Work [10] applies a Finite Control Set MPC (FCS-MPC) for voltage stabilization in grid-forming inverters of standalone AC microgrids. This inverter-level control enhances voltage quality and meets harmonic standards, but it does not address frequency regulation or system-wide coordination. Our approach extends beyond converter-level control by focusing on frequency stability at the microgrid level, achieving resilient operation under dynamic disturbances and load variations. While [11] presents a broad review of LFC strategies across various systems, our work focuses specifically on islanded microgrids, offering a predictive control solution that directly addresses their unique stability and uncertainty challenges. [12] presents a FOPI–FPOD controller optimized with multi-objective particle swarm optimization (PSO) to stabilize frequency in islanded microgrids, focusing on handling uncertainties like load changes and renewable energy fluctuations. While highlights improved stability through a multi-objective optimization process, our method emphasizes a real-time, model-based control strategy for more efficient frequency regulation in uncertain environments. [13] proposes a TIDA+1 controller optimized via a modified PSO for improving LFC in interconnected microgrids, focusing on offline parameter tuning and parallel signal correction. In contrast, our MPC-based method leverages a predictive model and real-time optimization to ensure dynamic, scenario-adaptive frequency regulation, offering greater flexibility and robustness under uncertainty. [14] presents a two-stage fuzzy controller optimized via PSO for enhancing LFC in renewable microgrids, focusing on fast dynamic responses and reduced energy storage dependence. In contrast, our MPC-based method uses predictive modeling and real-time optimization for scenario-adaptive frequency control, offering superior robustness against uncertainties. Voltage oscillation damping in DC microgrids is addressed by enhancing FCS-MPC with an active damping term tailored for constant power load stabilization [15]. Unlike our approach, which applies MPC in the AC domain for real-time frequency regulation under uncertainty, this work focuses on local converter-level voltage dynamics. Another study optimizes MPC parameters using a genetic algorithm to enhance frequency control in isolated microgrids, focusing on mitigating fluctuations from renewable intermittency and load disturbances [16]. While both approaches leverage MPC, our method integrates real-time adaptability without relying on offline GA tuning, offering faster responsiveness to dynamic uncertainties. Additionally, our controller ensures robustness across varying scenarios through predictive modeling rather than static parameter optimization. Conventional methods often rely on Proportional-Integral (PI) and Proportional-Integral-Derivative (PID) controllers, with tuning based on classical Ziegler-Nichols methods [17] and fractional-order techniques [18]. These approaches are utilized for microgrid LFC in studies such as [19]. Additionally, robust control strategies including $H\infty$ methods [20], advanced evolutionary algorithms [21], and D-K iteration-based designs [22] have been proposed. Droop control techniques have also been explored, ranging from linear [23] to nonlinear variations and those incorporating controllable loads. Sliding Mode Control (SMC) methods have been implemented using observers to further improve dynamic response [24]. Metaheuristic approaches for LFC have shown promise in addressing the nonlinear and uncertain nature of microgrid dynamics. Genetic Algorithms (GA) [18], Particle Swarm Optimization (PSO) [25], Social Spider Optimization (SSO) [26], Biogeography-Based Optimization (BBO) for PID tuning [27], and Harmony Search Algorithms [28] have been applied with success. Fuzzy logic systems, especially those enhanced with PSO or Type-2 logic, are also reported to be effective [29]. Furthermore, the secondary control of power converters in renewable energy sources has been considered for frequency regulation [30], and flexible scheduling of electric vehicles has been explored to enhance system resilience and operational flexibility [31]. Among advanced control methods, Model Predictive Control (MPC) stands out due to its ability to predict system behavior and optimize control actions accordingly [32]. Classical MPC [33], two-level MPC architectures [34], and coordinated MPC strategies integrating Electric Vehicles (EVs) [35] have all been explored to manage microgrid power and frequency fluctuations.

In summary, the reviewed literature underscores the diversity of existing LFC strategies and the growing emphasis on predictive and intelligent control frameworks. However, many approaches remain limited in adaptability, real-time optimization, or generalizability across heterogeneous microgrid configurations. These gaps motivate the development of the robust, scenario-adaptive MPC-based frequency control method proposed in this paper.

1.3. Challenge gap

Despite the progress in both classical and intelligent control methods, maintaining frequency stability in islanded microgrids under dynamic and uncertain conditions remains a major technical obstacle. Renewable energy sources are inherently intermittent, and the non-linear, time-varying nature of microgrid parameters further complicates controller design. Many conventional and heuristic approaches suffer from performance degradation in the face of such uncertainties, particularly when operating conditions deviate significantly from nominal values. Moreover, while MPC has shown significant potential, few studies have implemented it within a unified framework that integrates accurate modeling of various renewable sources, disturbance rejection, and performance benchmarking against well-established control schemes under both normal and uncertain conditions.

1.4. Novelty and main contributions

This paper presents a novel Load Frequency Control (LFC) strategy based on Model Predictive Control (MPC) for islanded microgrids incorporating diverse renewable energy sources such as photovoltaic panels, wind turbines, fuel cells, and energy storage systems. The proposed controller operates within the secondary control layer, where it applies optimized control signals to the renewable generation units to regulate frequency in the presence of load disturbances and system uncertainties. The proposed strategy is grounded in a small-signal state-space modeling framework, where the nonlinear dynamics of microgrid components are linearized around a steady-state operating point. This modeling approach allows accurate predictive control design, incorporating system constraints and enabling real-time optimization of control actions. The key contributions of this work are as follows:

- Development of a robust MPC-based control strategy tailored specifically to mitigate frequency oscillations in islanded microgrids. The predictive controller is designed with appropriate control and prediction horizons and is capable of operating under physical constraints on both control inputs and system responses.
- Integration of detailed state-space models derived from the linearization of dynamic behavior of renewable sources, enabling accurate representation of system dynamics for the control algorithm.
- Simulation-based validation using MATLAB/Simulink under five diverse operational scenarios. These scenarios evaluate the controller's performance under:
  o Sudden variations in renewable power generation (PV and wind)
  o Step and severe load disturbances
  o System parameter uncertainties introduced via the H(2) robustness metric
- Comparative analysis with classical and intelligent controllers, including ZN-PI, Fuzzy-PI, FOPID, PSOPID, CPSO-PID, and CPSO-FOPID. Results across all test cases demonstrate that the proposed MPC controller offers:
  o Faster damping of frequency oscillations
  o Lower overshoot and steady-state error
  o Enhanced robustness against disturbances and parametric variations
- Improved real-world applicability by addressing both dynamic frequency regulation and robustness needs, thus making the proposed method a strong candidate for practical deployment in next-generation microgrids with high renewable penetration.

In conclusion, this work contributes a systematically validated and practically oriented MPC-based LFC approach, advancing the reliability and stability of islanded microgrids under complex and variable operating conditions. Furthermore, unlike many traditional and heuristic LFC approaches that require offline parameter tuning and lack real-time adaptability, the proposed MPC strategy enables real-time optimization through an efficient quadratic programming formulation with modest computational overhead. By leveraging linearized state-space models, the controller maintains tractable computation suitable for implementation on practical digital controllers and embedded systems. This balance between predictive accuracy, adaptability, and computational feasibility makes the proposed method a strong candidate for real-world deployment in next-generation microgrids with high renewable penetration.

1.5. Organization of the paper

The remainder of this paper is structured as follows: Section 2 introduces the general structure of the microgrid and describes the existing control strategies, along with the dynamic modeling of each microgrid component. Section 3 details the design and mathematical formulation of the proposed Model Predictive Controller (MPC), including its cost function, constraints, and state-space implementation tailored for microgrid applications. Section 4 presents the simulation results, implementation outcomes, and comparative performance analysis of the MPC against traditional controllers. Section 5 concludes the paper by summarizing the key findings and outlining potential directions for future research.

2. General Microgrid Structure and Existing Control Strategy

This section presents the structure and design methodology of the proposed model predictive controller (MPC) used for secondary frequency control in the islanded microgrid. The general principles of MPC are first introduced, including its cost function formulation and constraint handling. Subsequently, the MPC is customized for the microgrid context by incorporating system dynamics, disturbance modeling, and optimization logic tailored to manage predictable and unpredictable power fluctuations.

2.1. Microgrid configuration

Fig. 1 shows the graphic diagram of studied microgrid, operating in islanded mode. The microgrid incorporates a PV array, a DEG, a WTG, a FC, and two energy storing causes, namely a battery energy storage system (BESS) and a flywheel energy storage system (FESS), along with an electrolyzer (AE). The energy bases within the microgrid are associated to key AC bus via power electronic converters, which also serve to control the power injected by these sources into the bus. The small-signal model of each microgrid component is described as follows:

A) Wind turbine generator

Eq. (1) represents the wind turbine generator (WTG) dynamic model for small-signal analysis, while Eq. (2) provides its characteristic function. These equations are specifically designed to describe the dynamic behavior of the WTG in response to small-signal variations, such as changes in wind speed and network load [36].

$$\Delta P_{\mathrm{WTG}}(s) = \frac{k_{\mathrm{WTG}}}{T_{\mathrm{WTG}}s + 1} \cdot \Delta P_{\mathrm{W}}(s) \tag{1}$$

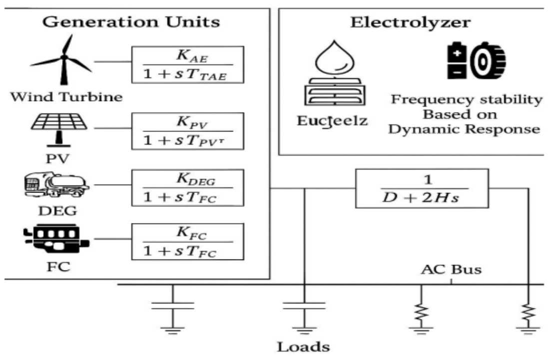

Fig. 1. Simple diagram of energy sources in the microgrid [5].

$$k_a = \frac{P_{\mathrm{WTG}}}{P_{\mathrm{W}}} \tag{2}$$

In Eqs. (1) and (2), k_{WTG} and T_{WTG} represent the gain and time constant of the wind turbine generator, respectively, k_a stands a constant indicating the ratio of the wind turbine power delivered to the microgrid, ΔP_{WTG} represents the variations in the WTG's output electrical power, and ΔP_{W} represents the variations in wind influence. The mined wind power (P_W) is achieved as:

$$P_{\mathrm{W}} = 0.5 \cdot \rho \cdot A_r \cdot C_P \cdot V_w^3 \tag{3}$$

In Eq. (3), C_P stands turbine power constant, ρ stays air density (kg/m^3), A_r stands swept zone of blades (m^2), and V_w stands wind velocity (m/s).

B) Photovoltaic (PV) array

The active typical of the PV array in small-signal examination is presented using Eqs. (4) and (5). In these equations, k_{PV} represents the gain of the photovoltaic array, and T_{PV} is its time constant. Variations in the PV array's output electrical power are denoted by ΔP_{PV}, and variations in solar irradiance are denoted by $\Delta\varphi$. The electrical power generated by the PV array, P_{PV}, is obtained using Eq. (6), which considers solar irradiance and the structural characteristics of the PV array [37].

$$\Delta P_{PV} = k_{PV} \cdot \Delta\phi \cdot \frac{1}{T_{PV}} P_{PV} = C_{PV} \cdot \pi \cdot A_r \cdot V_w \tag{4}$$

$$\Delta P_{PV}(t) = \frac{k_{PV}}{T_{PV}} \int_0^t (\Delta\phi(\tau) - \Delta P_{PV}(\tau))d\tau \tag{5}$$

$$P_{\mathrm{PV}} = \eta \cdot S \cdot \phi \cdot (1 - \beta(T_a - 25)) \tag{6}$$

In this equation, η is the efficiency of the PV array, S is the area of the PV array (m^2), φ is the solar irradiance (kW/m^2), T_a is the ambient temperature ($^\circ C$), and β is the temperature coefficient. For a more accurate analysis of this model, careful attention should be paid to the influence of environmental and operational variables on the output power of the PV arrays, as well as the impact of changes in solar irradiance and operational variations on electrical power. This model can be effectively used for dynamic simulations of microgrids and optimization of renewable energy system performance.

C) Diesel generator

The diesel generator serves as a key component in islanded hybrid microgrids. It assumes a serving of the power source responsibility needed to achieve power equilibrium when load demand increases. The model of the diesel generator [38] using Eqs. (7) and (8). These equations are a function of the diesel generator's output power and its dynamic characteristics, which can be used to simulate the system's behavior under various load and network conditions. These dynamic models play an important role in designing control and energy management strategies in microgrids.

$$\Delta P_{DEG} = k_{DEG} \cdot \Delta P - k_{DEG} \cdot F \cdot P_{DEG} P_{DEG}(s) = \frac{k_{DEG}}{C_{DEG} \cdot G_{DEG}(s) + sT_{DEG} \cdot U(s) + F(s) \cdot U(s) \cdot P_{DEG}(s)} \tag{7}$$

$$G_{\mathrm{DEG}}(s) = \frac{k_{\mathrm{DEG}}}{T_{\mathrm{DEG}} s + 1} \tag{8}$$

In these equations, ΔP_{DEG} represents variation in diesel generator output power. k_{DEG} is a constant related to the diesel generator. F is the characteristic function of the generator. P_{DEG} is the power generated by the diesel generator. T_{DEG} is the time constant of the diesel generator. $G_{DEG}(s)$ represents the dynamic performance of the system. $U(s)$ is the input function of the system. C_{DEG} is a constant associated with the diesel generator.

D) Electrolyzer (AE)

A portion of power produced by the wind turbine generator is used to power the electrolyzer. Eq. (9), which is used in the dynamic model of the electrolyzer for small-signal examination, has a characteristic function found in Eq. (10) [39]. These models are used to analyze the behavior of electrolyzer systems under various load conditions and variations in the input power to the system.

$$\Delta P_{AE} = k_{AE} \cdot \Delta P_{WTG} \tag{9}$$

$$P_{AE}(s) = \frac{k_{AE}}{C_{AE} \cdot G_{AE}(s) + sT_{AE} \cdot U(s) + F(s) \cdot U(s) \cdot P_{AE}(s)} \tag{10}$$

In the equations above, ΔP_{AE} represents the change in the electrolyzer power, which is supplied from a portion of the power generated by the wind turbine generator. The constant k_{AE} specifies the dynamic coefficients associated with the electrolyzer. ΔP_{WTG} represents the change in the wind turbine generator's output power, which affects the input of the electrolyzer. $P_{AE}(s)$ is the electrolyzer output power as a function of time. The parameter T_{AE} is the time constant of the electrolyzer, which indicates the time required for the system to reach a steady state. $G_{AE}(s)$ is a function that models the dynamic response of the electrolyzer. Also, $U(s)$ and $F(s)$ are the inputs and characteristics of the characteristic function of the electrolyzer system, respectively, which are used in modeling its behavior under various load and power input conditions. The constant C_{AE} is also a system parameter that considers the effects of other components of the system on the performance of the AE.

E) Fuel cell

In dynamic model of FC, variations in output electrical power ΔP_{FC} are modeled as a small signal using Eqs. (11) and (12). The parameters k_{FC} and T_{FC} are gain and time continuous of the FC, respectively, and their impact on the dynamic response of the system is considered. These models are designed to analyze the performance of the fuel cell under various load and power input conditions.

$$\Delta P_{FC} = k_{FC} \cdot \Delta P_{AE} - \frac{T_{FC}}{s} \cdot \Delta P_{FC} \tag{11}$$

$$P_{FC}(s) = \frac{k_{FC}}{1 + T_{FC}s} \cdot \Delta P_{FC} \tag{12}$$

F) BESS and FESS

Energy storage systems, such as batteries and flywheels, are used as key components in microgrids for load management and energy storage. Batteries and flywheels store excess power generated by renewable energy sources and effectively use it to supply energy during peak load times and power shortages. In this section, the dynamic models of these systems in small-signal analysis are examined in detail. The battery system model is described using Eqs. (13) and (14), and the flywheel system model is described using Eqs. (15) and (16) [40]. In these equations, the parameters k_{BESS} and T_{BESS} are the increase and time constant of battery organization, respectively, and k_{FESS} and T_{FESS} are the gain and time constant of FESS, respectively. Also, the changes in power generated or engaged from the battery and flywheel, and the control signals applied to these systems are also included in the models.

$$\Delta P_{BESS} = K_{BESS} \cdot \Delta U_{BESS} - \frac{T_{BESS}}{s} \cdot \Delta P_{BESS} \tag{13}$$

$$P_{BESS}(s) = \frac{K_{BESS}}{1 + T_{BESS}s} \cdot \Delta P_{BESS} \tag{14}$$

$$\Delta P_{FESS} = K_{FESS} \cdot \Delta U_{FESS} - \frac{T_{FESS}}{s} \cdot \Delta P_{FESS} \tag{15}$$

$$P_{FESS}(s) = \frac{K_{FESS}}{1 + T_{FESS}s} \cdot \Delta P_{FESS} \tag{16}$$

G) Microgrid frequency and power variations

Power variations in the microgrid directly affect frequency variations. An increase or decrease in power within the system causes changes in the microgrid's frequency, which is particularly noticeable during load changes or variations in energy inputs from renewable sources. The model of the microgrid for small-signal examination and simulation of these variations is expressed using Eq. (17). This model shows how power variations affect the microgrid's frequency and its response to these variations, which is of great importance in analyzing the performance and stability of hybrid microgrids.

$$\Delta F(s) = \frac{SY(s)}{SY(s)+SY(s)\cdot(1-K(s)T(s))+M(s)D(s)\cdot\Delta P(s)} \tag{17}$$

In this equation, $\Delta F(s)$ represents the frequency variations in the microgrid, S, $Y(s)$, $K(s)$, $T(s)$, $M(s)$, and $D(s)$ are various parameters of the microgrid system, and $\Delta P(s)$ is the power variation injected into the microgrid. This equation shows how power variations affect the microgrid frequency and is used for dynamic analysis of power systems.

$$\Delta F(s) = \frac{G(s)}{(1 + sT_M + D)} \Delta P(s) \tag{18}$$

In this equation, G(s) is the system transfer function, T_M is the equivalent time constant of the entire system, D is the damping coefficient, and $\Delta P(s)$ is the power variation of the system in per-unit (pu). The value of $\Delta P(s)$ is determined using Eqs. (19) and (20) [41]:

$$\Delta P(s) = \Delta P_{\text{WTG}}(s) + \Delta P_{\text{PV}}(s) + \Delta P_{\text{DEG}}(s) + \Delta P_{\text{FC}}(s) + \Delta P_{\text{BESS}}(s) + \Delta P_{\text{FESS}}(s) + \Delta P_{\text{AE}}(s) \tag{19}$$

$$\Delta P(s) = -R \cdot \Delta F(s) \tag{20}$$

As observed in Fig. 2, the occurrence of a disturbance in the microgrid and the disruption of power balance lead to frequency variations. In order to restore the frequency to its nominal value, control is performed at two distinct levels: primary frequency control and secondary frequency control [42].

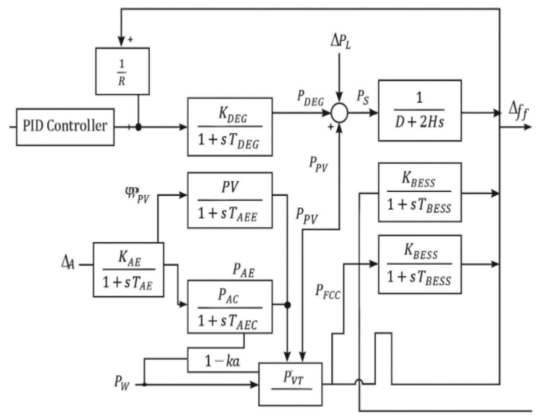

Fig. 2. Dynamic model of the microgrid.

1) Primary frequency control

As observed in Fig. 2, in micro grid under study, main frequency controller is completed through the droop loop of the diesel generator. This control is are defined as follows this Equation, where R is the droop coefficient in per-unit (pu) [41].

$$\Delta P_{\text{DEG}} = -R \cdot \Delta F$$

2) Secondary frequency control

The frequency drop is limited by primary frequency control, but it cannot be brought back to its nominal value. Consequently, a second control loop known as secondary frequency control is employed for accurate frequency regulation and to return it to its nominal value. This paper uses a model-based predictive controller in secondary controller loop to stabilize and regulate the frequency to its nominal value, as shown in Fig. 2.

To provide a comprehensive view of the implementation process of the Model Predictive Controller (MPC), the algorithm's operational structure is depicted in Fig. 3. This flowchart systematically illustrates the MPC algorithm used for secondary frequency control in the islanded microgrid. As shown, the process begins by measuring the current system state, including frequency, voltage, and power. These measurements are used to update the internal prediction model, typically based on system dynamics derived from small-signal state-space equations of the microgrid components.

Next, prediction and control horizons are set, and a cost function is formulated to penalize deviations from reference outputs and excessive control efforts. This cost function is minimized under the constraints of system inputs (e.g., actuator limits), input rate limits, and—if applicable output constraints. The resulting optimization problem is solved at each time step using quadratic programming (QP) or other appropriate solvers to obtain the optimal control signal sequence. However, only the first value of this sequence is applied to the system—a core feature of the receding horizon approach. This process repeats at every time instant, thereby continuously updating the control inputs in real time.

The structured sequence shown in Fig. 3 effectively supports secondary frequency control by reacting promptly to both predictable and unpredictable disturbances in power flow, thus helping restore frequency to its nominal value after deviations.

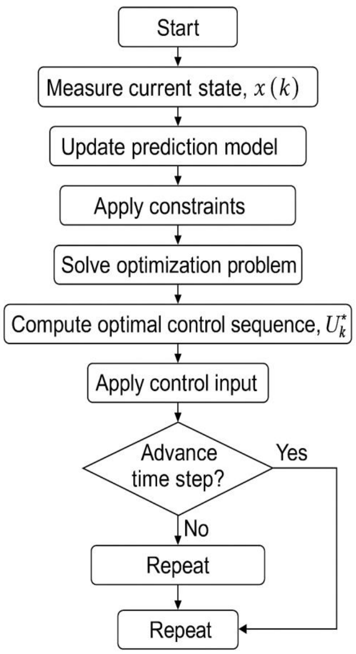

Fig. 3. Flowchart of the MPC algorithm implementation for secondary frequency control.

3. Model Predictive Controller (MPC)

This section presents the structure and design methodology of the proposed model predictive controller (MPC) utilized for secondary frequency control in the islanded microgrid. The general principles of MPC are initially introduced, including its cost function formulation and constraint handling. Following this, the MPC is customized for the microgrid context by integrating system dynamics, disturbance modeling, and optimization logic specifically designed for predictable and unpredictable power fluctuations.

3.1. General structure

MPC has been widely adopted in a broad spectrum of industrial applications, including chemical procedures, the oil industry, and electromechanical organizations. The general structure of this controller is depicted in Fig. 4. In this approach, a mathematical model of the system is used to predict and control its future behavior. The controller operation is based on minimizing a cost function, which enables the optimization of the control signal. The control signal is determined over a control horizon such that the system output follows a desired reference trajectory during the predicted time frame.

To achieve this goal, the cost function must be minimized. In this control method, a mathematical model of the system is used to predict its future behavior, and control is applied accordingly. The control signal is determined in such a way that a cost function is minimized. Optimizing this cost function ensures that the system follows the desired trajectory in the prediction horizon. The cost function used is defined in Eq. (21), while Eqs. (22) and (23) express the constraints imposed on the control signals and the system output. Eq. (21) expresses the cost function as follows [43]:

$$J = \sum_{j=1}^{N_p} \beta_j [y_{\mathrm{ref}}(k+j) - y(k+j)]^2 + \sum_{j=1}^{N_c} \lambda_j [u(k+j-1)]^2 \tag{21}$$

The constraints on the control signal and system output are defined as follows:

$$u_{\min} < u(k) < u_{\max} \tag{22}$$

$$y_{\min} \leq y(k) \leq y_{\max} \tag{23}$$

In which $u(k)$ is the control signal value at time k, $y(k)$ is the system output value at time k, u_{min} and u_{max} are the lower and upper bounds of the control signal, respectively, and y_{min} and y_{max} are the lower and upper bounds of the system output, respectively.

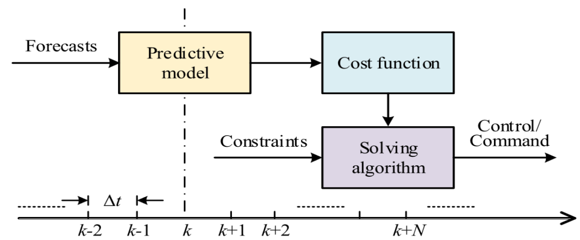

Fig. 4. General structure of the model predictive controller [44].

The weighting factor (βj) serves as weighting coefficients for the error, and (λj) serves as weighting coefficients for the control signal in the cost function of the predictive controller. These coefficients production and significant role in determining the importance of each of the controlled variables and control signals in the optimization process. Fig. 5 shows the timing of the calculation of the control signals and how they are obtained.

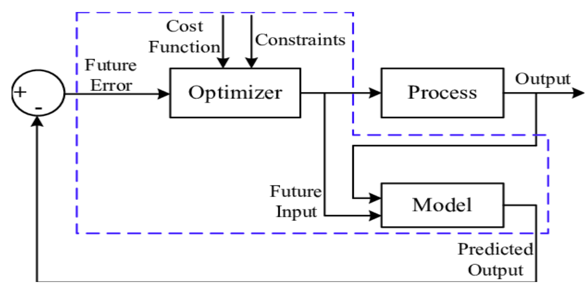

Fig. 5. Timing of signals in the predictive controller.

3.2. MPC design

Frequency fluctuations are caused by changes in the power produced by the microgrid's sources and load. There are two types of microgrid power sources:

a) The flywheel, battery storage system, and diesel generator are examples of controllable sources.

b) Uncontrollable sources: such as solar cells, wind turbines, and fuel cells. Variations in load are viewed as unpredictable disturbances in the predictive controller design, while variations in uncontrollable power sources are regarded as predictable disturbances. The structure and input/output signals of the suggested microgrid predictive controller are depicted in Fig. 6.

The state-space equations of the predictive controller are as:

$$X(k+1) = A \cdot X(k) + B \cdot U(k) + D \cdot W(k) \tag{24}$$

In Eq. (24), X and A are state variable vector and state-space matrix, U stands controller output, B stands constant matrix, W stands disturbance input, and D stands disturbance matrix.

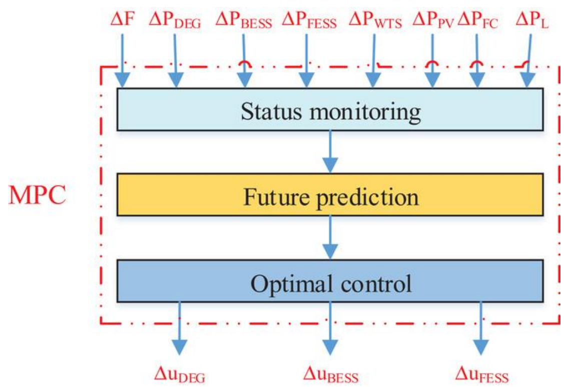

Fig. 6. Structure of the suggested predictive microgrid controller [45].

First, changes in power bases, load, and microgrid frequency are assessed and measured in the suggested controller (as shown in Fig. 6). The next step involves predicting the system output (variations in frequency) and applying the proper controller signals in accordance with predetermined guidelines. Eqs. (25) through (32) provide the following description of the relationships controlling the controller's behavior [45]:

$$J = \sum_i (\delta_i \cdot u_i)^2 \tag{25}$$

$$u(k+1) = u(k) + \sum_i \delta_i \tag{26}$$

$$u_{\min} \leq u(k+1) \leq u_{\max} \tag{27}$$

$$0 \leq \beta_j \leq 1 \tag{28}$$

$$0 \leq \lambda_j \leq 1 \tag{29}$$

$$U = [u_1, u_2, ..., u_{N_c}]^T \tag{30}$$

$$Js = \sum_{k=0}^{N} \left(\beta_k \cdot (y(k) - y_{\text{ref}}(k))^2 + \lambda_k \cdot (u(k))^2\right) \tag{31}$$

$$U = f(\Delta P_{\text{BESS}}, \Delta P_{\text{FESS}}, \Delta P_{\text{DEG}}) \tag{32}$$

The set of control signals (Eq. (30)) is obtained by minimizing the objective function, which is Eq. (25) and is modified as a quadratic program. The signals at each time step are calculated using Eq. (26). Numerical coefficients denoted as δ_i are derived from the problem's solution (by minimizing J). The least and extreme ranges of the applied controller signal at every time stage are displayed in Eq. (27). The variety of the chosen constants in objective function are displayed in Eqs. (28) and (29) respectively. The state variables at each time step are calculated using Eq. (31) and the control signals taken into account for the energy storage sources are displayed in Eq. (32). Also, in the calculations, the following index is obtained:

$$\text{IAE} = \sum_{k=1}^{N} |y(k) - y_{\text{ref}}(k)| \tag{33}$$

In this equation, $y(k)$ represents the system output and $y_{ref}(k)$ represents the reference output value. The control strategies in the simulation section are compared using the index shown in Eq. (33). In addition to controlling the microgrid frequency, the predictive controller must also use the power source converters and the diesel generator excitation system to control and regulate the microgrid voltage level. A different subject that is outside the purview of this work is how to regulate the microgrid's voltage.

4. Simulation Results

Before presenting the detailed simulation results, it is important to clarify that the equations and transfer functions used in Sections 2 and 3 are derived from established models and validated references, primarily based on sources [46] and [47]. These references provide standard parameter values, dynamic models, and transfer function definitions commonly used in power system control studies. The diagrams and figures introduced in those sections were either adapted from these references or developed using MATLAB/Simulink based on the referenced system configurations. This foundation ensures that the simulation results presented in the following subsections are built upon well-established and scientifically supported modeling approaches.

4.1. Microgrid model setup and controller parameters

As detailed in Section 3, the microgrid simulation incorporates various types of renewable energy sources. These sources include photovoltaic systems, wind turbines, fuel cells, and other renewable energy technologies, which are used to supply energy to the microgrid. Each of these energy sources has its own specific characteristics and parameters, which significantly affect the system performance in the simulation. The precise values of these parameters, including energy production capacity, efficiency, charge and discharge rates of energy storage systems, and other technical specifications, are listed in Table 1. These parameters have been accurately adjusted based on experimental data and standard values from reputable sources [46].

This simulation is performed to evaluate the behavior of the microgrid under various load conditions and energy disturbances. In this model, renewable energy sources are continuously capable of supplying the system's energy needs under varying load conditions and different environmental conditions. On the other hand, changes in the frequency and voltage of the microgrid are also precisely controlled to ensure the necessary coordination between energy sources and consumers in the microgrid.

Table 1. Microgrid system parameters and transfer functions [46].

Constraint	Rate	Constraint	Rate
D (pu/Hz)	0.013	T_{WTG}	1.25
H (pu·s)	0.1657	T_{AE}	0.25
T_{FES}	0.1	K_{WTG}	1
T_{BES}	0.1	R (Hz/pu)	5
T_{FC}	4	K_t	0.6
K_{FC}	1.200	K_{DEG}	1.5
K_{AE}	1.300	K_{FESS}	-0.01
K_{BESS}	-0.0433	K_{PV}	1
T_{DEG}	2	T_{PV}	1.8

The Model Predictive Control parameters are set as follows:

- $N_p = 1$ (Prediction horizon)
- $N_c = 2$ (Control horizon)
- $N_u = 2$

In these parameters, the weight values on the manipulated variables are set as follows:

- Weight on manipulated variables: 0
- Weight on rate of change of manipulated variables: 0.1
- Weight on output signal: 0 to 2

- Sampling time: 0.0002 seconds

The maximum and minimum values of the control signal ($u_{\min} \leq u(k) \leq u_{\max}$) are set as follows:

- $u_{max} = 1$ pu
- $u_{min} = 0.1$ pu
- Maximum frequency deviation: 1 pu
- Minimum frequency deviation: -1 pu

Table 2. Pseudo code for shuffled bat optimization algorithm.

$G_{FC(s)}$	$\frac{K_{FC}}{T_{FC}s+1}$
$G_{PV(s)}$	$\frac{K_{PV}}{T_{PV}s+1}$
$G_{AE(s)}$	$\frac{K_{AE}}{T_{AE}s+1}$
$G_{BESS(s)}$	$\frac{K_{BESS}}{T_{BESS}s+1}$
$G_{FESS(s)}$	$\frac{K_{FESS}}{T_{FESS}s+1}$
$G_{DEG(s)}$	$\frac{K_{DEG}}{T_{DEG}s+1}$
$G_{WTG(s)}$	$\frac{K_{WTG}}{T_{WTG}s+1}$
CPV	$CPV = \eta \cdot A \cdot G$ (Efficiency × Area × Irradiance)

To ensure that the selected Model Predictive Control (MPC) parameters are optimal, a sensitivity analysis was performed by testing multiple combinations of prediction horizon (N_p) and control horizon (N_c). The configurations evaluated included ($N_p = 1,\ N_c = 2$), ($N_p = 2,\ N_c = 2$), ($N_p = 3,\ N_c = 3$), and ($N_p = 1,\ N_c = 1$). The evaluation criteria included the Integral of Time-weighted Absolute Error (ITAE), maximum frequency deviation, and settling time under identical disturbance conditions. The configuration with $N_p = 1$ and $N_c = 2$ demonstrated the best overall performance, achieving minimal frequency deviation (0.0052 pu), shortest settling time (5.1 s), and lowest ITAE (0.00024). Increasing the prediction and control horizons did not significantly improve performance but did increase computational complexity. Conversely, reducing them degraded frequency regulation quality. Therefore, the selected MPC parameters ($N_p = 1,\ N_c = 2$) strike an effective balance between dynamic performance and computational efficiency in microgrid control.

4.2. Controller performance evaluation under disturbances

To evaluate the performance of the proposed control method, simulations were conducted using MATLAB/Simulink. Disturbances applied to the microgrid (sudden load changes and variations in distributed generation sources) are shown in Figs. 7-9. The disturbance in Fig. 7 corresponds to a change in photovoltaic power, Fig. 8 corresponds to a change in wind turbine influence, and Fig. 9 corresponds to a variation in the micro grid load [46].

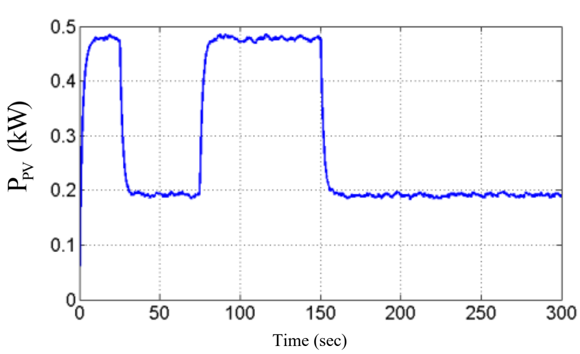

Fig. 7. Change in photovoltaic power [46].

The simulation results were analyzed in detail across five different scenarios to evaluate the performance of the various control methods under different microgrid conditions. In each scenario, the performance of the different controllers was evaluated based on their ability to damp frequency oscillations and respond to various disturbances.

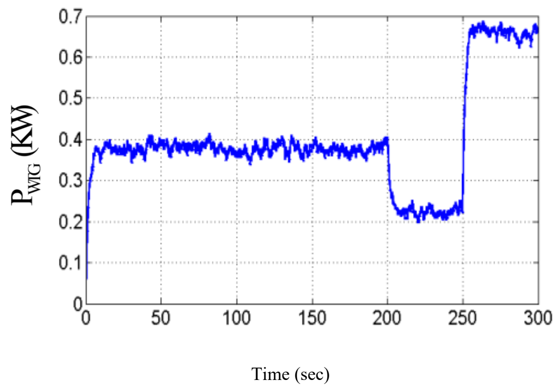

Fig. 8. Change in wind turbine power [46].

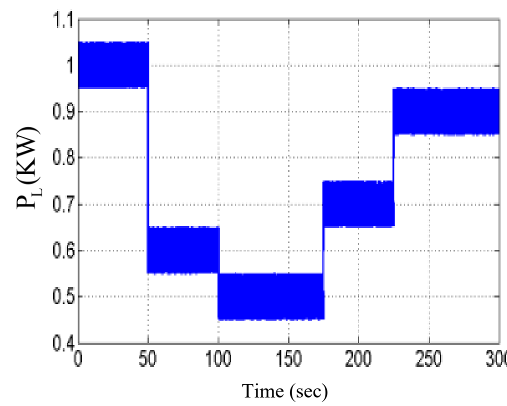

Fig. 9. Microgrid load variations [46].

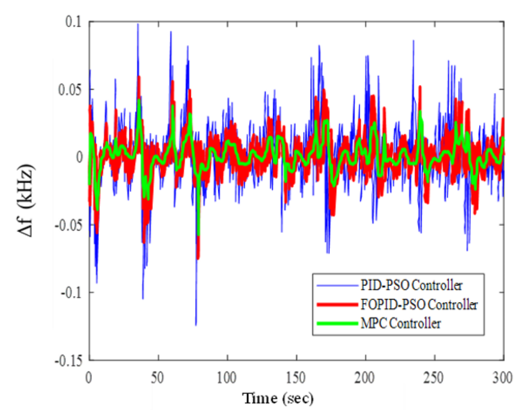

Fig. 10. Controller performance for damping frequency variations in scenario 1.

Scenario 1: In this scenario, the performance of three controllers (CPSO-FOPID, CPSO-PID, and the proposed controller) was investigated. Simultaneous disturbances, such as changes in the power of distributed generation sources (including photovoltaic, wind turbine, and microgrid load), were applied to the system. The results showed that the proposed controller performed better than the two controllers CPSO-FOPID and CPSO-PID in damping frequency oscillations in the microgrid. This was particularly

Table 3. Controller performance based on index in scenarios 4 and 5.

Scenario	ZN-PI [47]	Fuzzy-PI [47]	MPC controller
4	0.000137	0.0002	0.00024
5	0.00109	0.00272	0.00426

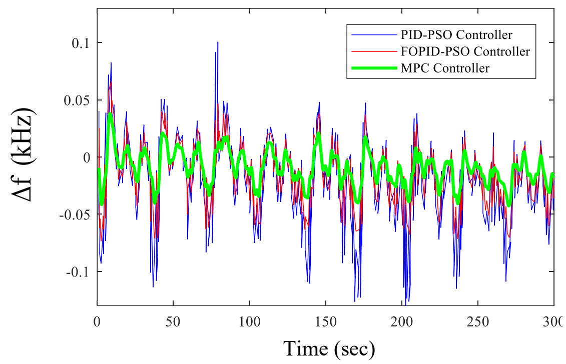

Fig. 11. Controller performance for damping frequency variations in scenario 2.

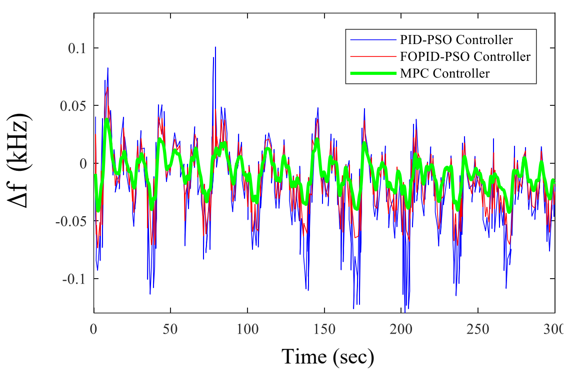

Fig. 12. Controller performance for damping frequency variations in scenario 3.

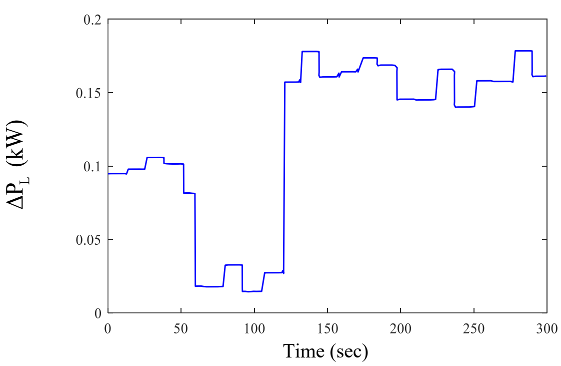

Fig. 13. Step load disturbance.

evident in reducing the amplitude of frequency overshoots and undershoots, as well as reducing the number of oscillations. The proposed controller was able to effectively maintain the microgrid frequency within the desired range and prevent excessive oscillations. These results indicate the higher efficiency of this controller against disturbances, which can improve the stability and reliability of the microgrid system in real-world operating environments.

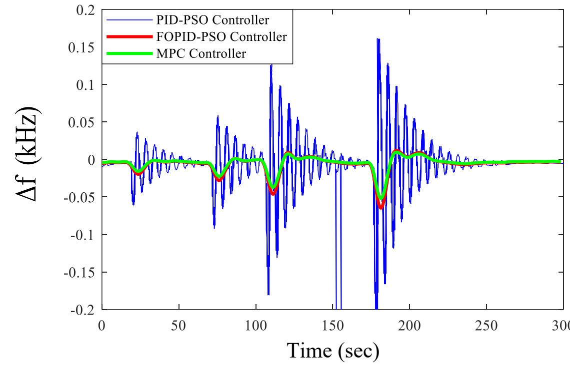

Fig. 14. Performance of different controllers for damping frequency in scenario 4.

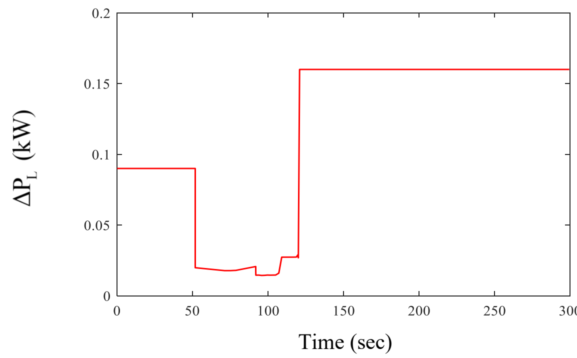

Fig. 15. Relatively severe step load disturbance.

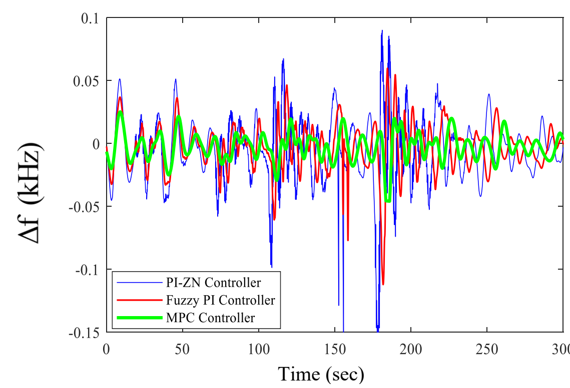

Fig. 16. Performance of different controllers for damping frequency in scenario 5.

Scenario 2: In this scenario, similar to the first scenario, but with the addition of a new robustness parameter (H(2)) to the controllers in order to examine performance under conditions of system parameter variations. In this scenario, the parameter H(2) was varied in the range $[1.5 \times 10^{-3},\ 5.1]$. These changes in the parameter allowed the evaluation of controller results under conditions resistant to disturbances. The results of this scenario also showed that the proposed controller performed better than the two controllers CPSO-FOPID and CPSO-PID in the face of these parametric changes and frequency oscillations. In this scenario, even with changes in the parameters, the proposed controller was able to maintain the microgrid frequency accurately and with minimal oscillations, which demonstrates its robust and adaptable characteristics.

Table 4. Comparative economic analysis of control strategies.

Criterion	ZN-PI controller [47]	Fuzzy-PI controller [47]	Proposed MPC controller
Initial setup cost	Low	Moderate	High
Maintenance cost	Moderate	High	Low
Tuning complexity	Low	Moderate	High
Computational load	Low	Moderate	High
Disturbance handling ability	Low	Moderate	High
Frequency stability achieved	Moderate	Moderate	High
Operational efficiency	Moderate	Moderate	High
Long-Term cost efficiency	Moderate	Low	High

The simulation results clearly demonstrate the high efficiency of the proposed controller in improving the frequency stability of the microgrid under various disturbance conditions. This controller not only provided a desirable response to frequency oscillations but also remained robust and reliable against changes in system parameters. This can be useful in the design and implementation of control systems for future microgrids, especially in environments with complex and unpredictable disturbances.

Scenario 3: Similar to Scenario 1, but to estimate robust enactment of controllers, it is supposed that H(2) can vary in range $[1.5 \times 10^{-3},\ 5.1]$. In this scenario, the response of the controllers to simultaneous disturbances is shown in Fig. 12. The results show that the proposed controller performs better than the other controllers in this case as well. This is especially observed in conditions where system parameter variations occur. The proposed controller in this scenario is able to maintain the stability of the microgrid frequency with better performance in damping oscillations.

Scenario 4: In this scenario, a disturbance of the type of step load changes according to Fig. 13 is applied to the microgrid. To compare the response of different controllers, the renewable energy source parameters presented in [47] are used in scenarios 4 and 5. Fig. 14 shows the performance of the ZN-PI, Fuzzy-PI, and proposed controllers. In this scenario, the results show that the performance of the proposed controller is significantly better than the other controllers. In particular, the proposed controller was able to damp frequency oscillations better than the other controllers and ultimately create better stability in the microgrid.

Scenario 5: The conditions are similar to Scenario 4, but the disturbance applied to the microgrid is a relatively severe step load disturbance, as shown in Fig. 15. In this scenario, the performance of the proposed controller and the ZN-PI and Fuzzy-PI controllers for damping frequency variations is shown in Fig. 16. The results show that the performance of the proposed controller in this scenario is also significantly more desirable than the other controllers. This demonstrates the better capability of the proposed controller in the face of severe disturbances and rapid load changes.

To better evaluate the proposed controller and compare it with the ZN-PI and Fuzzy-PI controllers, an index is defined according to Eq. (33). The evaluation results of the various controllers in Scenarios 4 and 5 are shown in Table 2. As can be seen in this table, the enactment of suggested controller is enhanced than the additional controllers. These results emphasize the advantages of using the proposed controller in microgrids, especially in conditions where there are severe disturbances and rapid dynamic changes.

4.3. Economic analysis of controller implementation

In addition to technical performance, the economic feasibility of implementing the proposed MPC-based controller is a critical consideration. Table 4 compares the MPC controller with traditional control strategies in terms of implementation cost, maintenance, tuning complexity, and system benefits. While the MPC strategy involves a higher initial setup and computational demand, the long-term benefits, such as improved stability, fewer operational losses, and lower maintenance costs, justify the investment, especially in complex microgrid environments that experience frequent disturbances.

Table 4 supports the conclusion that although the MPC controller may incur higher upfront costs and tuning efforts, it provides superior economic value in the long run through robust control, reduced instability-related losses, and improved energy balance.

5. Conclusion and Future Work

Frequency control is a fundamental requirement in maintaining the stability and performance of islanded microgrids, especially those with high penetration of renewable energy sources. In this study, a robust Model Predictive Control (MPC)-based Load Frequency Control (LFC) strategy was proposed and evaluated for a diverse microgrid system composed of photovoltaic (PV), wind turbine generator (WTG), fuel cell (FC), battery energy storage system (BESS), flywheel energy storage system (FESS), diesel engine generator (DEG), and aqua electrolyzer (AE) units.Extensive simulations using MATLAB/Simulink demonstrated the superior performance of the proposed controller in mitigating frequency oscillations compared to classical and intelligent controllers such as PI-ZN, Fuzzy-PI, CPSO-PID, and CPSO-FOPID. Quantitatively, the proposed MPC controller achieved a maximum frequency deviation of only 0.0052 pu, a settling time of 5.1 seconds, and an ITAE of 0.00024, significantly outperforming other methods in terms of stability and responsiveness. Five distinct disturbance scenarios were examined, including step load changes and parameter uncertainties. For example, in Scenarios 4 and 5, which involved moderate to severe step disturbances, the proposed controller achieved performance indices of 0.00024 and 0.00426, respectively, while outperforming the benchmark ZN-PI and Fuzzy-PI controllers. Furthermore, a sensitivity analysis on the controller parameters confirmed that the selected values ($N_p = 1$, $N_c = 2$) provide an effective trade-off between control performance and computational demand. Economically, although the MPC-based controller requires a higher initial setup and tuning complexity, it offers substantial long-term benefits such as improved operational efficiency, better disturbance rejection, and reduced maintenance costs. These characteristics make it a compelling solution for real-world microgrid applications, especially in systems subject to high levels of dynamic uncertainty.

Future research can focus on extending the proposed control framework to hybrid AC/DC microgrids and incorporating adaptive MPC algorithms that can self-tune under varying system conditions. In addition, integrating machine learning techniques for disturbance prediction and multi-objective optimization can further improve control precision and economic performance. Hardware-in-the-loop (HIL) testing and experimental validation on a real-time digital simulator (RTDS) platform are also recommended to assess practical feasibility and deployment readiness.

References

[1] R. Prakash and S. S, "Optimal distributed generation planning considering economic and operational aspects," *Electr. Power Compon. Syst.*, vol. 52, no. 9, pp. 1581–1596, 2024.

[2] M. Rezaee, R. Fathi, and V. A. Maleki, "Dynamic analysis and uncertainty modeling of viscoelastic beam response to fluid stimulation: Insights into nonlinear effects and velocity uncertainties," *Appl. Ocean Res.*, vol. 157, p. 104487, 2025.

[3] N. Sharafkhani, J. O. Orwa, S. D. Adams, J. M. Long, G. Lissorgues, L. Rousseau, and A. Z. Kouzani, "An intracortical polyimide microprobe with piezoelectric-based stiffness control," *J. Appl. Mech.*, vol. 89, no. 9, p. 091008, 2022.

[4] S. Pirouzi, M. Zadehbagheri, and S. Behzadpoor, "Optimal placement of distributed generation and distributed automation in the distribution grid based on operation, reliability, and economic objective of distribution system operator," *Electr. Eng.*, pp. 1–14, 2024.

[5] M. Abbasi, E. Abbasi, L. Li, R. P. Aguilera, D. Lu, and F. Wang, "Review on the microgrid concept, structures, components, communication systems, and control methods," *Energies*, vol. 16, no. 1, p. 484, 2023.

[6] A. Younesi, H. Shayeghi, and P. Siano, "Assessing the use of reinforcement learning for integrated voltage/frequency control in ac microgrids," *Energies*, vol. 13, no. 5, p. 1250, 2020.

[7] K. H. M. Azmi, N. A. M. Radzi, N. A. Azhar, F. S. Samidi, I. T. Zulkifli, and A. M. Zainal, "Active electric distribution network: applications, challenges, and opportunities," *IEEE Access*, vol. 10, pp. 134655–134689, 2022.

[8] S. Kiani, A. Salmanpour, M. Hamzeh, and H. Kebriaei, "Learning robust model predictive control for voltage control of islanded microgrid," *IEEE Trans. Autom. Sci. Eng.*, 2024.

[9] C. Zhong, H. Zhao, Y. Liu, and C. Liu, "Model predictive secondary frequency control of island microgrid based on two-layer moving-horizon estimation observer," *Appl. Energy*, vol. 372, p. 123721, 2024.

[10] Q. Ullah, E. C. Resende, L. C. G. Freitas, H. Laaksonen, and M. G. Simões, "Enhancing voltage stability of grid forming power converters based on model predictive controller," *Int. J. Electr. Power Energy Syst.*, vol. 163, p. 110317, 2024.

[11] H. Shayeghi, H. A. Shayanfar, and A. Jalili, "Load frequency control strategies: A state-of-the-art survey for the researcher," *Energy Convers. Manage.*, vol. 50, no. 2, pp. 344–353, 2009.

[12] H. Shayeghi, A. Rahnama, and H. Mojarad, "Designing a multi-objective optimized parallel process controller for frequency stabilization in an islanded microgrid," *J. Oper. Autom. Power Eng.*, 2025.

[13] H. Shayeghi, A. Rahnama, N. Bizon, and A. Szumny, "Interconnected microgrids load-frequency control using stage-by-stage optimized tida+1 error signal regulator," *Eng. Rep.*, vol. 7, no. 1, p. e13095, 2025.

[14] H. Shayeghi, A. Rahnama, and N. Bizon, "Green microgrid's lfc using recursive step-by-step optimized multi-stage fuzzy controller with separated inference systems," *Renew. Energy Focus*, vol. 51, p. 100625, 2024.

[15] R. Kumar and C. N. Bhende, "Voltage oscillations stabilization in dc microgrids: A strategy using improved model predictive control," *IEEE J. Emerg. Sel. Top. Power Electron.*, 2024.

[16] A. K. Tudu, N. Naguru, S. H. N. Dey, and S. Paul, "Load frequency control of an isolated microgrid using optimized model predictive control by ga," *Electr. Eng.*, vol. 106, no. 4, pp. 4171–4183, 2024.

[17] C. I. Muresan and R. De Keyser, "Revisiting ziegler–nichols: A fractional order approach," *ISA Trans.*, vol. 129, pp. 287–296, 2022.

[18] S. Othman, N. Sunar, A. Ismail, M. Ayob, M. M. Azmi, and M. Hashim, "Position tracking performance with fine tune ziegler-nichols pid controller for electro-hydraulic actuator in aerospace vehicle model," *J. Phys. Conf. Ser.*, vol. 2021, p. 012021, 2021.

[19] M. Nasrabadi and L. Hussein, "Designing the optimal energy damping suspension system with the method of least displacement and genetic algorithm," *Procedia Environ. Sci. Eng. Manage.*, vol. 10, no. 3, pp. 469–476, 2023.

[20] P. K. Ray, H. K. Sahoo, A. Mohanty, J. K. Bhutto, A. B. Barnawi, and A. A. Alshaya, "Robust h-infinity filter and pso-svm based monitoring of power quality disturbances system," *IEEE Access*, vol. 12, pp. 39041–39057, 2024.

[21] Y. Zou, J. Qian, Y. Zeng, S. Ismail, F. Dao, Z. Feng, C. Nie, and H. Mei, "Optimized robust controller design based on cpsogsa optimization algorithm and h2/h∞ weights distribution method for load frequency control of micro-grid," *IEEE Access*, vol. 9, pp. 162093–162107, 2021.

[22] P. S. Prasad and A. M. Parimi, "Robust μ-synthesis controller design and analysis for load frequency control in an ac microgrid system," *IFAC-Pap. Online*, vol. 55, no. 1, pp. 547–554, 2022.

[23] M. R. Ghodsi, A. Tavakoli, and A. Samanfar, "A robust controller design for load frequency control in islanded microgrid clusters," *Int. Trans. Electr. Energy Syst.*, vol. 2022, no. 1, p. 4218067, 2022.

[24] M. Ramesh, A. K. Yadav, P. K. Pathak, and C. H. Basha, "A novel fuzzy assisted sliding mode control approach for frequency regulation of wind-supported autonomous microgrid," *Sci. Rep.*, vol. 14, no. 1, p. 31526, 2024.

[25] T. M. Shami, A. A. El-Saleh, M. Alswaitti, Q. Al-Tashi, M. A. Summakieh, and S. Mirjalili, "Particle swarm optimization: A comprehensive survey," *IEEE Access*, vol. 10, pp. 10031–10061, 2022.

[26] J. Wang, "Optimizing support vector machine (svm) by social spider optimization (sso) for edge detection in colored images," *Sci. Rep.*, vol. 14, no. 1, p. 9136, 2024.

[27] X. Li, J. Chen, D. Zhou, and Q. Gu, "A modified biogeography-based optimization algorithm based on cloud theory for optimizing a fuzzy pid controller," *Optim. Control Appl. Methods*, vol. 43, no. 3, pp. 722–739, 2022.

[28] F. Qin, A. M. Zain, and K.-Q. Zhou, "Harmony search algorithm and related variants: A systematic review," *Swarm Evol. Comput.*, vol. 74, p. 101126, 2022.

[29] M. H. Khooban, T. Niknam, F. Blaabjerg, and T. Dragičević, "A new load frequency control strategy for micro-grids with considering electrical vehicles," *Electr. Power Syst. Res.*, vol. 143, pp. 585–598, 2017.

[30] S. Ahmad, M. Shafiullah, C. B. Ahmed, and M. Alowaifeer, "A review of microgrid energy management and control strategies," *IEEE Access*, vol. 11, pp. 21729–21757, 2023.

[31] A. Younesi, Z. Wang, H. T. Nguyen, and P. Mandal, "A pathway to enhance the modern distribution systems resilience: Flexible behavior investigations on electric vehicles," in *Proc. IEEE Power Energy Soc. Gen. Meet.*, pp. 1–5, 2022.

[32] M. Schwenzer, M. Ay, T. Bergs, and D. Abel, "Review on model predictive control: An engineering perspective," *Int. J. Adv. Manuf. Technol.*, vol. 117, no. 5, pp. 1327–1349, 2021.

[33] K. S. Joshal and N. Gupta, "Microgrids with model predictive control: a critical review," *Energies*, vol. 16, no. 13, p. 4851, 2023.

[34] B. Khokhar and K. S. Parmar, "A novel adaptive intelligent mpc scheme for frequency stabilization of a microgrid considering soc control of evs," *Appl. Energy*, vol. 309, p. 118423, 2022.

[35] B. Khokhar, S. Dahiya, and K. P. S. Parmar, "Load frequency control of a multi-microgrid system incorporating electric vehicles," *Electr. Power Compon. Syst.*, vol. 49, no. 9-10, pp. 867–883, 2021.

[36] A. Tabesh and R. Iravani, "Small-signal dynamic model and analysis of a fixed-speed wind farm—a frequency

response approach," *IEEE Trans. Power Del.*, vol. 21, no. 2, pp. 778–787, 2006.

[37] M. Carrasco, F. Mancilla-David, and R. Ortega, "An estimator of solar irradiance in photovoltaic arrays with guaranteed stability properties," *IEEE Trans. Ind. Electron.*, vol. 61, no. 7, pp. 3359–3366, 2013.

[38] J. V. Knudsen, "Modeling, control, and optimization for diesel-driven generator sets," 2017.

[39] M. S. Genc, M. Celik, and I. Karasu, "A review on wind energy and wind–hydrogen production in turkey: A case study of hydrogen production via electrolysis system supplied by wind energy conversion system in central anatolian turkey," *Renew. Sustain. Energy Rev.*, vol. 16, no. 9, pp. 6631–6646, 2012.

[40] M. Shen and Q. Gao, "A review on battery management system from the modeling efforts to its multiapplication and integration," *Int. J. Energy Res.*, vol. 43, no. 10, pp. 5042–5075, 2019.

[41] T. John and S. P. Lam, "Voltage and frequency control during microgrid islanding in a multi-area multi-microgrid system," *IET Gener. Transm. Distrib.*, vol. 11, no. 6, pp. 1502–1512, 2017.

[42] H. Bevrani, *Robust Power System Frequency Control*, vol. 4. Springer, 2014.

[43] A. H. Glattfelder and W. Schaufelberger, *Control Systems with Input and Output Constraints*, vol. 1. Springer, 2003.

[44] J. Hu, Y. Shan, J. M. Guerrero, A. Ioinovici, K. W. Chan, and J. Rodriguez, "Model predictive control of microgrids – an overview," *Renew. Sustain. Energy Rev.*, vol. 136, p. 110422, 2021.

[45] S. M. S. Hussain, A. Latif, M. A. Aftab, C. Konstantinou, A. Al-Durra, and M. A. Abido, "Standardized communication-based diverse structure model predictive controller with demand response for frequency regulation in microgrids," *IEEE Trans. Ind. Appl.*, vol. 60, no. 2, pp. 3554–3567, 2023.

[46] I. Pan and S. Das, "Fractional order agc for distributed energy resources using robust optimization," *IEEE Trans. Smart Grid*, vol. 7, no. 5, pp. 2175–2186, 2015.

[47] H. Bevrani, F. Habibi, P. Babahajyani, M. Watanabe, and Y. Mitani, "Intelligent frequency control in an ac microgrid: Online pso-based fuzzy tuning approach," *IEEE Trans. Smart Grid*, vol. 3, no. 4, pp. 1935–1944, 2012.